

# Ballistic-to-diffusive transition in spin chains with broken integrability

João S. Ferreira<sup>1</sup> and Michele Filippone<sup>1</sup>

<sup>1</sup>*Department of Quantum Matter Physics, University of Geneva,  
24 Quai Ernest-Ansermet, CH-1211 Geneva, Switzerland*

(Dated: May 25, 2022)

We study the ballistic-to-diffusive transition induced by weakly breaking integrability in the boundary-driven XXZ spin-chain. Studying the evolution of the spin current density  $\mathcal{J}^s$  as a function of the system size  $L$ , we find that the transition has a non-trivial universal behavior close to the XX limit. In the XXZ model, integrability breaking leads to strong linear corrections in the finite-size scaling of the current. These corrections destroy the universal scaling observed in the XX model. Furthermore, they control the emergence of a “quasi-ballistic” regime at length scales much shorter than those expected from Fermi’s golden rule. Our results are based on Matrix Product Operator numerical simulations and agree with perturbative analytical calculations.

PACS numbers: 02.30.Ik, 66.10.Cb

## I. INTRODUCTION

A central assumption of statistical mechanics is that many-body interactions bring isolated out-of-equilibrium systems towards thermal equilibrium [1–4]. The phenomenon of thermalization in normal - metallic - conductors is generally associated with diffusion. Globally conserved quantities such as energy, charge, spin or mass spread uniformly all over the system according to Fick’s law

$$\mathcal{J} = -D\nabla n, \quad (1)$$

in which the diffusion constant  $D$  relates the current density  $\mathcal{J}$  to the application of a density gradient  $\nabla n$ . Recently, it has been observed that in one-dimension, quantum integrable systems defy thermalization [5]. This discovery has triggered an intense effort to understand the non-trivial dynamics of such systems under the recently developed framework of generalized hydrodynamics [6, 7]. In particular, the presence of an extensive amount of conservation laws in integrable systems [8] generically leads to ballistic transport of conserved quantities [9]. An important exception is the XXZ model, which can show, for some choice of the model parameters, (sub)diffusive behavior [10–13].

Unavoidable deviations from the realization of a perfect, fine-tuned integrable system lead to integrability breaking (IB). In that case, one typically expects the slow establishment of a chaotic-diffusive regime on time scales given by Fermi’s golden rule (FGR) [14, 15]. Nevertheless, the investigation on how IB triggers proper diffusive regimes for transport remains at a preliminary stage. Even though recent works [16–18] derived a generalized expression of FGR to describe diffusive hydrodynamics caused by integrability breaking, the onset of diffusion may still unveil highly non-trivial behavior [19, 20]. Additionally, the onset of chaotic/diffusive behavior, for fixed weak interactions is not controlled by Fermi’s golden rule at small system sizes [21–23]. Recent works have also pointed out that the emergence of chaotic/diffusive behavior may not be fully related to the usual measure-

ments of quantum chaos, such as level repulsion [24–26] or the eigenstate thermalization hypothesis [27].

Quantum quenches are a very efficient and widespread protocol used to study the relaxation dynamics of such many-body systems [28–35]. They are regularly performed in state-of-the-art cold-atom experiments [36–39] and can be efficiently simulated by numerical approaches [40–44]. Nevertheless, the description of the long-time dynamics driven by weak IB remains challenging for the available analytical and numerical studies.

We chose to address this issue from a different but complementary point of view. We investigate at which system *sizes* do weak and moderate IB interactions of strength  $V$  lead to a ballistic-to-diffusive transition. We study the effect of next-to-nearest neighbor interactions on the stationary current carried by a ballistic XXZ spin-chain driven at its boundaries, see Fig. 1. The boundary terms induce a bias in the magnetization that in turn generates a spin current density,  $\mathcal{J}^s$ . This approach has

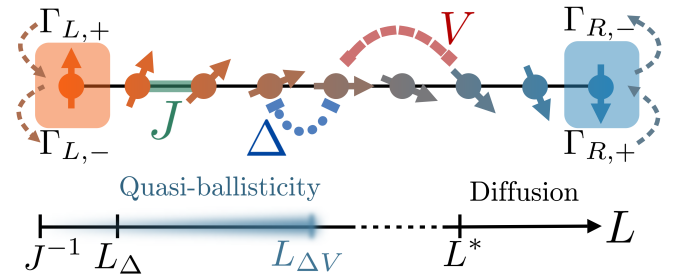


Figure 1. Top) System under study: a spin current is induced via biased Lindblad jump operators at the edge of a XXZ spin chain described by Eq. (2). Bottom) Schematic behavior of the steady-state current as a function of the system size  $L$ . The ballistic (size-independent) regime in the XXZ model sets in after the length scale  $L_\Delta$ . Breaking integrability triggers diffusion beyond the scattering length  $L^*$ , given by Fermi’s golden rule. The ballistic-to-diffusive crossover regime is controlled by the emerging length scale  $L_{\Delta V} \ll L^*$ , which defines a parametrically large “quasi-ballistic” regime.

the advantage to directly probe the stationary properties of highly excited many-body systems with large system sizes [12, 45].

In the case of the XX non-interacting limit with IB perturbations, we find that the current deviates from ballistic behavior as a universal function of the system size  $L$ . Because of finite size-effects, this universal scaling is not a trivial function of  $L/L^*$  as suggested from FGR, where  $L^* \propto V^{-2}$  is the scattering length. Also, this universal scaling allows the precise extrapolation of the diffusion constant up to moderately large interaction strengths  $V$ .

We then extend to the study of the integrable ballistic case in the presence of interactions ( $|\Delta| < 1$ ). Here, we show the emergence of *linear* terms in the IB strength  $V$ . These terms have strong qualitative effects on the stationary current, before the onset of diffusion. In the  $V \rightarrow 0$  limit, these linear corrections trigger unexpected manifestations of IB on a parametrically large length scale  $L \leq L_{\Delta V} \propto V^{-1}$ , much shorter than the expected scattering length  $L^*$ . For systems smaller than  $L_{\Delta V}$ , IB leads to a “quasi-ballistic” regime, where the current remains constant, see Fig. 1. For repulsive interactions ( $V > 0$ ), the current may be even increased, with respect to the integrable case.

The results in this paper are expected to manifest themselves in real experiments probing the transport [46–48] and relaxation properties of isolated interacting systems, close to integrable points.

Our paper is structured as follows. In Section II, we present the system, the Lindblad formalism, which allows to describe a stationary state carrying a current and the numerical approach based on tDMRG. In Section III, we discuss the universal scaling induced by IB when perturbing the XX limit. Section IV discusses the effect of IB in the XXZ model. We show the emergence of strong deviations to the stationary current which depend on the sign of the strength of the IB term and illustrates the existence of a parametrically large quasi-ballistic regime. Section V is devoted to the discussions of our results and conclusions. The appendices incorporate details about the tDMRG implementation, perturbation theory and complementary plots to our numerical analysis.

## II. MODEL AND METHODS

We consider the anisotropic Heisenberg (XXZ) chain in one dimension [49]

$$\mathcal{H}_{\text{XXZ}} = J \sum_{i=1}^{L-1} (\sigma_i^x \sigma_i^x + \sigma_i^y \sigma_i^y) + \Delta \sum_{i=1}^{L-1} \sigma_i^z \sigma_{i+1}^z, \quad (2)$$

in which  $\sigma^{x,y,z}$  are the standard Pauli matrices and  $L$  the number of spins in the system. Using the Jordan-Wigner transformation, Eq. (2) maps to a chain of spinless fermions with hopping amplitude  $2J$  and nearest-neighbor interactions of strength  $4\Delta$ . For practical reasons, we will use the spin formulation of the problem in

the remainder of the paper and set  $J = 1$ . The model (2) is integrable and its ground state is gapless for  $\Delta \in [-1, 1]$  and gapped otherwise. Remarkably, it supports ballistic spin transport at finite energy density in the gapless phase [11], subdiffusion at the isotropic point  $|\Delta| = 1$  and normal diffusion otherwise [10, 12].

Transition to a diffusive regime is expected when breaking integrability. For the remainder of the paper, we explicitly break integrability by adding global next-to-nearest neighbor (NNN) interactions

$$\mathcal{H}_{\text{NNN}} = V \sum_{i=1}^{L-2} \sigma_i^z \sigma_{i+2}^z. \quad (3)$$

To study transport, we numerically mimic the experimentally relevant situation [46–48] in which the system is coupled at its two ends to a left (L) and a right (R) magnetization reservoir. If there is a small magnetization bias, it induces a non-equilibrium steady state (NESS) carrying spin current, see Fig. 1. Coupling to external (Markovian) reservoirs results in a non-unitary evolution of the system’s density matrix  $\rho$ . We simulate this evolution with the Lindblad master equation [50, 51]

$$\frac{d\rho}{dt} = -i[\mathcal{H}, \rho] + \sum_{\substack{\alpha=L,R \\ \tau=\pm}} 2\Gamma_{\alpha\tau} \rho \Gamma_{\alpha\tau}^\dagger - \{\rho, \Gamma_{\alpha\tau}^\dagger \Gamma_{\alpha\tau}\}. \quad (4)$$

The dissipative dynamics induced by the reservoirs is expressed in terms of the jump operators  $\Gamma_{\alpha\tau} = \sqrt{\gamma(1 + \tau\mu_\alpha)} \sigma_\alpha^\tau$ , where  $\gamma$  is the injection/loss rate and  $\mu_L = -\mu_R = \frac{\delta\mu}{2}$ , with  $\delta\mu$  being the bias in magnetization, see also Fig. 1. To simplify the expressions, we fix  $\gamma = 1$ . For small magnetization bias,  $|\delta\mu| \ll 1$ , the NESS induced by Eq. (4) is close to the infinite temperature state,  $\rho_\infty = \mathbb{I}^{\otimes L}/2^L$ . The stationary state carries a non-zero average spin-current density  $\mathcal{J}^s = \langle \hat{\mathcal{J}}^s \rangle$ , in which  $\hat{\mathcal{J}}^s = 2 \sum_i^L [\sigma_i^+ \sigma_{i+1}^- - \text{h.c.}]/L$  is the corresponding current density operator.

The biased jump operators  $\Gamma_{\alpha\tau}$  enforce different spin densities at the two ends of the chain [52] and allow for a direct investigation of the spin-current. In particular, the dependence of the spin current  $\mathcal{J}^s$  as a function of system size  $L$  allows us to distinguish between ballistic and diffusive transport regimes. Ballistic regimes are not described by Fick’s law (1) and they are characterized by a steady-state current that does not decay with system size  $L$ , whereas diffusive regimes are signaled by a current which decays inversely with  $L$ .

### A. Numerical methods

To find the steady-state of the master equation (4), we employ a time-dependent density matrix renormalization-group (tDMRG) method [40], implemented with the ITensor library [53]. For  $\delta\mu = 0$ , the

steady-state of Eq. (4) is the infinite temperature state. We thus perform a real-time evolution of an initial density matrix  $\rho(t=0) = \rho_\infty = \mathbb{I}^{\otimes L}/2^L$ , which is written in a matrix product operator (MPO) form. Since the non-equilibrium steady state,  $\rho_{\text{NESS}} = \lim_{t \rightarrow \infty} \rho(t)$ , is unique, it is well approximated by  $\rho(t)$  for very large times and increasing bond dimensions. By numerically verifying convergence both in time and bond dimension, we are able to compute the NESS for system sizes up to one-hundred sites ( $L = 100$ ). Our numerical simulations were carried out for a magnetization bias  $\delta\mu = 0.1$ , for which we verified that the current's response is linear in  $\delta\mu$ . The bond dimension is limited to  $\chi = 160$  and the time step of the Trotter decomposition ranges from  $dt = 0.05$  to  $dt = 0.2$ . The interested reader is redirected to App. A, where we provide all the necessary details concerning our numerical simulations.

### III. IB AND XX MODEL ( $\Delta = 0$ ) THE UNIVERSAL CROSSOVER TO DIFFUSION

For the XX chain ( $\Delta = V = 0$ ), the MPO expression of the steady-state of Eq. (4) has been derived in Ref. [54, 55], and found to carry a ballistic spin current  $\mathcal{J}^s = \delta\mu$  [56]. Interactions such as Eq. (3) induce inelastic scattering among free-particles, which leads to a decay of the spin current and the onset of diffusion in the thermodynamic limit.

For finite but large systems, the ballistic-to-diffusive transition is marked by a sizable deviation from  $\mathcal{J}^s = \delta\mu$  at a crossover length scale  $L^*$ . According to FGR, this scattering length is expected to scale as  $L^* \sim V^{-2}$  in the  $V \rightarrow 0$  limit.

We numerically derive the evolution of the current, as a function of the system size  $L$ , for different strengths  $V$  of the NNN interaction, Eq. (3). Such evolution is shown in the inset of Fig. 2. As expected, with increasing strength of the IB parameter  $V$ , the current decreases monotonically for a fixed length  $L$  and diffusion sets in at smaller  $L$ .

According to FGR, one would expect that the current satisfies a scaling hypothesis controlled by the scattering length, i.e.  $\mathcal{J}^s/\delta\mu = \mathcal{F}(L/L^*) = \mathcal{F}(LV^2)$ . However, such scaling ansatz does not allow a perfect collapse of all the numerical curves onto a unique function, see Fig. 6 in App. B. Instead, a universal scaling is only achieved when considering a non-trivial parameter  $V^2 f_{V^2}(L)$ , see Fig. 2. The collapse of the curves is excellent up to large system sizes and moderate IB strengths ( $V = 0.5$ ). For  $L > 5$ , the function  $f_{V^2}$  is linear with a non-zero offset value,  $f_{V^2}(L) \approx 0.40L - 1.35$  (see Fig. 8 in App. C). This offset is responsible for preventing a scaling with  $L/L^* \propto LV^2$  for small/intermediate system sizes. For larger system sizes, the offset becomes negligible and  $L^*$  correctly captures the ballistic-to-diffusive transition.

As a consequence of the universal scaling, the parameter  $f_{V^2}(L)$  must appear in the expansion of the current

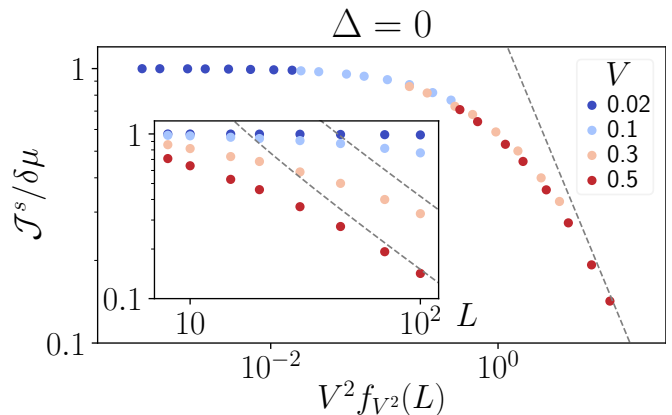


Figure 2. Scaling dependence of  $\mathcal{J}^s$  in the XX model for different strengths  $V$  of the next-nearest neighbors interaction (3) as a function of the scaling parameter  $V^2 f_{V^2}(L)$ . In the inset, the same quantity as a function of the system size  $L$ . The dashed gray lines are fits to the diffusive behavior scaling as  $1/L$ .

$\mathcal{J}^s$  for small IB strength  $V$ . Using perturbation theory, we show that

$$\mathcal{J}^s = \left[ 1 - V^2 f_{V^2}(L) + \mathcal{O}(V^4) \right] \delta\mu, \quad (5)$$

in the limit of  $V^2 f_{V^2}(L) \ll 1$ . We analytically computed the dependence on size  $L$  of the function  $f_{V^2}$ , as shown in Fig. 8 in App. C.

The divergence of the correction of order  $V^2$  in Eq. (5) signals the transition to the diffusive regime. In that regime, the numerics are consistent with the expression

$$\mathcal{J}^s = \frac{1.45}{V^2 f_{V^2}(L)} \delta\mu, \quad (6)$$

corresponding to the gray dashed lines in Fig. 2. For asymptotically large  $L$ , Eq. (6) acquires the form  $\mathcal{J}^s = D_{\Delta=0}^s \delta\mu/2L$ , in which  $D_{\Delta=0}^s \approx 7.3/V^2$  is the spin diffusion constant. This value of the diffusion constant is derived by considering the equivalent of Fick's law (1) in the spin formulation of the problem, namely  $\mathcal{J}^s = -D^s \nabla s^z = D^s \delta\mu/2L$ , in which  $s^z = \langle \sigma^z \rangle / 2$  is the spin expectation value. We have verified numerically, that  $\nabla s^z = -\delta\mu/2L$  gives the correct estimate of the spin-density gradient in diffusive regimes, see App. B. One should notice that a precise evaluation of  $D_{\Delta=0}^s$  for weak  $V$  would hardly be possible from the non-rescaled plots of Fig. (2), or without considering the correct scaling parameter, see Fig. 6 in App. B.

This discussion concludes our analysis of the ballistic-to-diffusive transition induced by IB on the XX model. We now extend to the interacting and integrable case, showing how nearest-neighbor interactions of strength  $0 < \Delta < 1$ , strongly modify the effects of IB on the ballistic regime.

#### IV. IB AND XXZ MODEL WITH $|\Delta| < 1$

##### A. The ballistic, integrable regime

The sole presence of nearest-neighbor interactions does not hinder ballistic transport in the thermodynamic limit for  $|\Delta| < 1$  [11, 57, 58]. For finite systems, the current depends non-trivially on the system size. With increasing  $L$ , the current decreases monotonically until it saturates to its ballistic (thermodynamic) value. This saturation occurs beyond a typical length scale  $L_\Delta$  which depends on the strength  $\Delta$  of the integrable next-nearest interaction.

The behavior of  $\mathcal{J}^s$  as function of  $L$  is shown in Fig. 3, which reproduces the findings of Ref. [59] and that we display here for clarity. To our knowledge, the exact size dependence of the current is unknown. It is possible to obtain perturbatively the finite-size behavior of the current for  $\Delta \rightarrow 0$

$$\mathcal{J}^s = \left[ 1 - \Delta^2 f_{\Delta^2}(L) + \mathcal{O}(\Delta^2) \right] \delta\mu, \quad (7)$$

where  $f_{\Delta^2}$  is a linear function similar to  $f_{V^2}$ , see App. C. In analogy to the discussion of the previous section, Eq. (7) is only valid for system sizes  $L < L_{\Delta \ll 1} \propto 1/\Delta^2$ . Beyond  $L_{\Delta \ll 1}$ , perturbative results diverge linearly in  $L$  and miss the saturation of the current which, to be derived, would require the re-summation of the perturbation theory in  $\Delta$  to all orders. It should be stressed that, even though the expansions (5) and (7) look almost identical, their linear divergences do not signal analogous behaviors in the thermodynamic limit. In particular, in the non-integrable case, one would find the diffusive current suppression described by Eq. (6).

##### B. Strong linear effects induced by IB

We now study the transition to the diffusive regime induced by the IB term (3) for  $|\Delta| < 1$ . In Fig. 4, we present the size dependence of the spin current for  $\Delta = 0.3$  and different IB parameters.

Figure 4a shows the suppression of the current density for large systems and strong IB. The suppression is compatible with a diffusive scaling, see dashed grey lines. However, the observation of a clear diffusive behavior lays beyond the available system sizes. Thus we cannot conclude about the  $\Delta$ -dependence of the diffusion constant [60].

Nevertheless, the most striking and visible effect in the numerics is not the current suppression, but the strong sensitivity of  $\mathcal{J}^s$  to the sign of the coupling constant  $V$ . Such feature is absent in the non-interacting limit ( $\Delta = 0$ ). For certain sizes, the value of the current can even *increase* with respect to the integrable case after breaking integrability. This relative increase persists up to system sizes of the order of one-hundred sites and

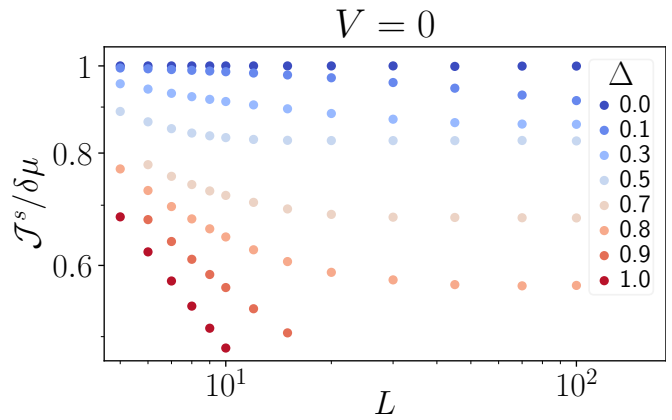


Figure 3. Finite size scaling of  $\mathcal{J}^s$  in the ballistic regime of the XXZ model (2), for different  $0 < \Delta < 1$ . For  $\Delta < 1$ , the current always saturates to a constant value signaling the ballistic regime.

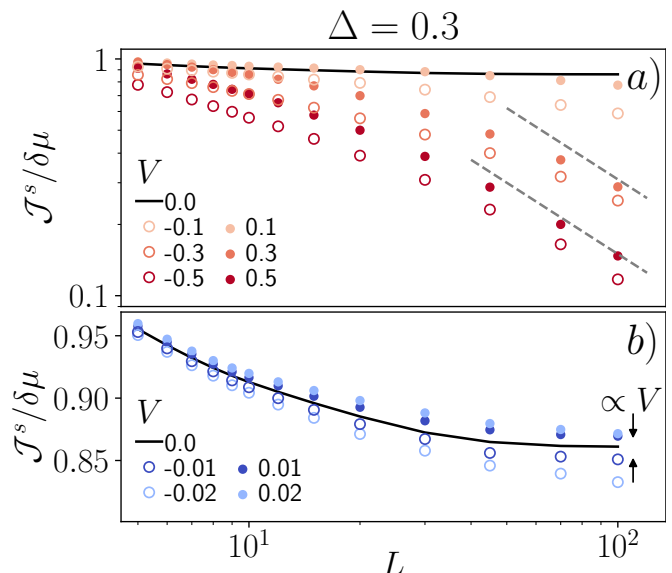


Figure 4. System-size dependence of the XXZ current in the presence of non-integrable interactions (3) and for different IB strengths  $V$ . In all cases we compare to the integrable ballistic case for  $\Delta = 0.3$  (solid black line). a) For moderately strong IB ( $|V| \geq 0.1$ ), at short system sizes, the stationary current is strongly sensitive to sign of the IB term  $V$  before the onset of diffusion, which is signaled by the dashed-gray at larger system sizes. b) Illustration of the quasi-ballistic regime in the  $V \rightarrow 0$  limit. For weak IB, the ballistic regimes appears to be just renormalized by linear (sign-dependent) corrections in  $V$ .

non-perturbative values of the IB strength  $V \sim 0.1$ , see Fig. 4a.

The limit  $V \rightarrow 0$  is particularly interesting. As apparent in Fig. 4b, IB appears to just renormalize the relaxation towards the ballistic regime and the saturation value of the current. As a consequence, IB has an effect on length scales much shorter than those controlling the

onset of diffusion at the scattering length scale  $L^*$ , given by FGR. Also in this case, the renormalization of the stationary current is clearly sensitive to the sign of the IB strength  $V$ .

This strong sensitivity of the current to the sign of the IB term  $V$  denotes the existence of linear effects in  $V$  whose fate is intriguing in the thermodynamic limit. In particular, concerning the renormalization of the ballistic regime observed in Fig. 4b. In the next section, we argue how linear corrections control the IB crossover to the diffusive regime, giving rise to an emergent “quasi-ballistic” regime.

### C. The “quasi-ballistic” regime

The perturbation theory carried out in the previous sections provides some insight into the nature of the linear correction in  $V$ . It arises as a second-order term in  $\Delta V$  when perturbing the current close to the XX limit. Similarly to the  $\Delta^2$  and  $V^2$  corrections, this contribution also diverges linearly with the system size  $L$ , see App. C. To understand whether the linear correction becomes dominant in the thermodynamic limit, we rely on a systematic study of the finite-size scaling of the current at finite  $\Delta$ . We numerically probe the  $V \rightarrow 0$  limit by assuming a polynomial expansion of the current:

$$\frac{\mathcal{J}^s}{\delta\mu} = 1 - c_0(\Delta, L) + V c_1(\Delta, L) - V^2 c_2(\Delta, L) + \mathcal{O}(V^3) \quad (8)$$

which extends Eqs. (5) and (7). Equation (8) is consistent with the perturbative result derived in App. C, where all these coefficients are calculated up to second order and found to diverge linearly with the system size  $L$ .

In Fig. 5a, we depict the dependence of the spin current  $\mathcal{J}^s$  on the IB perturbation strength  $V$  for finite  $\Delta = 0.3$  and increasing system sizes  $L$ . For  $V \ll \Delta$ , all curves are nicely fitted with expression (8), with  $c_i$  as free parameters. The asymmetry of the parabolic dependence on  $V$  is a clear indicator of the presence of linear corrections for  $\Delta \neq 0$ . In Figs. 5b-d, we show the obtained finite-size scaling of the coefficients  $c_i$  for different values of  $\Delta$ . The dashed lines correspond to the analytic predictions derived with perturbation theory in App. C. They show an excellent agreement with the numerics in the  $\Delta \rightarrow 0$  limit [61].

Figure 5c clearly shows that the coefficient  $c_1$ , which controls the linear corrections in  $V$ , behaves analogously to  $c_0$ , and thus saturates to finite values at systems sizes of the order of  $L_\Delta$ . This is not the case for the coefficient  $c_2$ , which controls the second-order corrections to  $\mathcal{J}^s$  in  $V$ . Its linear divergence as a function of  $L$  is only weakly affected by the presence of a finite  $\Delta$ . The fact that only the terms of order  $\mathcal{O}(V^2)$  diverge suggests that the diffusive regime is established at the scattering length  $L^* \sim 1/V^2$ , as expected by FGR [16–18]. This observation is consistent with the numerical simulations presented in Fig. 4a.

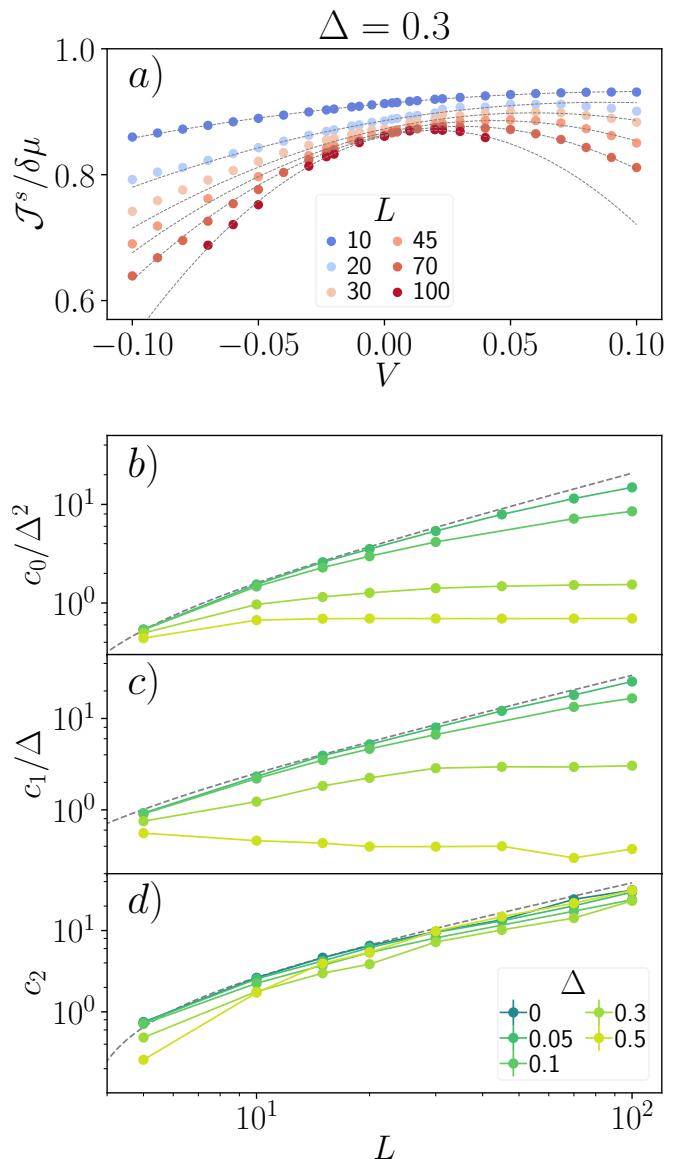


Figure 5. a) Dependence of  $\mathcal{J}^s$  for  $\Delta = 0.3$  and different system sizes, as a function of small IB parameters. Dashed lines represent the fitting functions of Eq. (8). b-d) System-size dependence of the fitting parameters for different  $\Delta$  parameters. The dashed-gray lines correspond to the predictions from second order perturbation theory. For small  $\Delta$ , the results approach the perturbative predictions.

The different size dependence of the coefficients  $c_1$  and  $c_2$  corresponds to strong qualitative effects of IB on integrable systems. First of all, the non-zero linear corrections in  $V$  signal that IB has prominent effects at system sizes much shorter than  $L^*$ . In contrast to the XX case, IB does not primarily lead to the inelastic scattering of quasi-particles and the onset of diffusion. Instead, IB leads to a “quasi-ballistic” regime in which the value of the ballistic current in the XXZ model is just renormalized by IB. Whether such corrections can be interpreted as a renormalization of the quasi-particle velocity is left

for future investigation.

Additionally, such quasi-ballistic regime persists up to a novel and parametrically large length scale  $L_{\Delta V}$ , which controls the onset of diffusion and is much shorter than  $L^*$ . An estimate of  $L_{\Delta V}$  can be obtained from Eq. (8). It is defined as the length scale at which the diverging term of order  $\mathcal{O}(V^2)$  dominates the linear correction of order  $\mathcal{O}(V)$ . For  $|V| \ll \Delta$ , we can define such length scale as

$$L_{\Delta V} \sim \frac{1}{|V|c_1(\Delta, L \rightarrow \infty)} \ll L^* \sim \frac{1}{V^2}. \quad (9)$$

This emergent length scale marks the system sizes up to which IB acts as a renormalization of the ballistic current of the integrable XXZ model with  $|\Delta| < 1$ . For system sizes  $L \simeq L_{\Delta V}$ , the deviations from the ballistic regime become sizable, and the crossover to diffusion starts. Remarkably, such length scale does not emerge from generalized hydrodynamics approaches [16–18]. The reason is that generalized hydrodynamics is a “coarse-grained” approach, which considers the limit  $L \rightarrow \infty$  before  $V \rightarrow 0$ . Our numerical and analytical predictions rely on the opposite order of limits, which will be relevant to study IB in real experiments. Nevertheless, we expect our effects to appear on the time-scales controlling the quantum evolution after quenches.

We conclude this section by stressing that the existence of such linear effects compromises the possibility to collapse the crossover to diffusion onto a unique, universal curve.

## V. CONCLUSIONS

In this work, we studied and characterized the effects of integrability-breaking on the spin current of a boundary-driven chain. We have first considered integrability breaking of the non-interacting XX chain. We showed that the crossover to diffusion is universal and controlled by a novel scaling parameter,  $V^2 f_{V^2}(L)$ , which we computed using perturbation theory. For large systems, it correctly recovers the expectation that diffusion is controlled by FGR via the scattering length  $L^* \sim V^{-2}$ . We have also shown that deviations from the ballistic behavior are only observed for system sizes of order  $L \sim L^*$ , as expected in free models.

Nevertheless, the fact that deviations from ballisticity in the XX model are controlled by second order corrections in the IB strength  $V$  is not trivial. In Ref. [22], the evolution of eigenstates in the presence of IB terms was studied exactly for the same model. In that work, it was pointed out that, for fixed system sizes  $L$ , perturbation theory is expected to fail for systems sizes  $\tilde{L} \propto V^{-1/2}$ . Such an estimate is readily derived by noticing that NNN interactions have typical matrix elements of order  $V/L$  which couple  $\rho \propto 1/L^3 \ln L$  states, because of total momentum conservation. Now, it is remarkable that the length scale  $\tilde{L}$  does not appear at all in the finite-size scaling of the current during the onset of diffusion. The

physical effects of such length scales pave the way to stimulating investigations concerning other effects of integrability breaking. It is also an interesting line of investigation to extend our approach to the regimes in which  $V$  is of the order, or larger, of the hopping  $J$ .

We have then addressed the effects of IB in the ballistic regime of the XXZ model. Our observations are consistent with the validity of Fermi’s golden rule in the diffusive regime, even though the precise determination of the diffusion constant in the presence of a finite  $\Delta < 1$  and  $V \rightarrow 0$  remains an interesting (and challenging) line of investigation [60]. Our main result is that IB controls the ballistic-to-diffusive transition in a non-trivial way for interacting models. Unlike the non-interacting XX case, we showed that linear corrections in  $V$  influence transport long before the onset of diffusion. As mentioned above, the physical meaning of such linear corrections still has to be clarified. We believe that they correspond to a renormalization of the quasi-particle’s effective velocity.

An interesting direction would be to compare and make the connection of our findings with the time-scales describing the relaxation of non-integrable quantum systems [24, 25]. For instance, by studying the unitary evolution of a weakly polarized domain-wall state [6, 7, 12, 35]. It would be important to understand the role of IB terms different from Eq. (3), such as disorder, single impurities [24, 25, 62] and also dephasing [63, 64].

Future research directions could address the propagation of energy and spin [65] in the presence of IB. In particular, whether the Wiedemann-Franz law [66] is restored in the presence of IB terms, since it is notoriously violated in such systems at low temperatures [20, 67–69]. An additional perspective is the investigation of different integrability perturbations and their effect on quantum ladder systems attached to reservoirs [70–72].

## ACKNOWLEDGMENTS

J. S. F. and M. F. acknowledge several discussions with Dmitry A. Abanin, Vincenzo Alba, Christophe Berthod, Thierry Giamarchi, Tony Jin and, in particular, with Marko Žnidarić during the whole realization of this work and support from the FNS/SNF Ambizione Grant PZ00P2\_174038. J.S.F acknowledges Miles Stoudenmire and Matthew Fishman for the helpful support with the ITensor library and thanks Michael Sonner and Sofia Azevedo for the careful reading of the manuscript.

## Appendix A: Numerical details

Except for the large coupling limit,  $V \rightarrow \infty$ , the models presented in the main text have a unique non-equilibrium steady state (NESS) in the thermodynamic limit. This condition ensures that we can reach the NESS via a real time-evolution  $\rho_\infty = \lim_{t \rightarrow \infty} \exp(\mathcal{L}t)\rho(0)$  of

any initial state  $\rho(0)$ . We initialize the state in the product state  $\rho(t=0) = \mathbb{I}^{\otimes L}/2^n$ .

For small systems,  $L < 8$ , we use exact diagonalization as baseline for other time-evolution methods. Beyond  $L = 8$ , we employ time-evolving block decimation (TEBD), which allows us to efficiently find the NESS of large spin chains,  $L \lesssim 100$ . The algorithm was first explored in Ref. [73] and consists of applying a Suzuki-Trotter decomposition of the Lindblad super-operator to the state  $\rho$ . In our case, we use a 4th order decomposition introduced in Ref. [74]. At any time during the time-evolution, the density matrix can be written in a matrix product operator form

$$\rho = \sum_{\{i\}} M_1^{i_1} M_2^{i_2} \dots M_L^{i_L} (\sigma_1^{i_1} \otimes \sigma_2^{i_2} \otimes \dots \otimes \sigma_L^{i_L}) \quad (\text{A1})$$

where we choose the local basis to be the Pauli matrices  $\sigma^{0,1,2} = \sigma^{x,y,z}$  and  $\sigma^3 = \mathbb{I}$  and  $\dim(M_k^i) = \chi \times \chi$ . In general, the application of non-unitary two-site gates leads to nonphysical states as it breaks the orthogonality condition assumed in TEBD. To avoid reorthogonalizing the MPO at every time-step, we apply the gates sequentially instead [75]. We simulate the next-to-nearest interaction using the swap-gate technique.

In the presence of interactions, the necessary bond dimension  $\chi$  to simulate the NESS is expected to grow with the system size. We consider that the time evolved state  $\rho(t)$  correctly approximates the NESS if it satisfies three criteria: the current is homogeneous across the chain, the average current does not evolve in time and the current converges as the bond-dimension increases. Next, we present the algorithm used in this paper. The quantity  $\bar{\mathcal{J}}$  represents the spatial average of the spin current

1. Initialize with the product state  $\rho(t=0) = \mathbb{I}^{\otimes L}/2^n$  ( $\chi_0 = 1$ )
2. Increase the bond-dimension by  $\chi_i = \delta\chi + \chi_{i-1}$ .
3. Time-evolve the state until the current has saturated in time.
  - (a) Compute the time variance in the last  $T = 10, 30$  time units (of hopping)  $\sigma_T^2 = \sum_{i=1}^T (\bar{\mathcal{J}}(t-i) - \mu)^2 / T$
  - (b) Repeat step 3 until  $|\sigma_{30}^2 - \sigma_{10}^2| / \sigma_{30}^2 < 1\%$
4. Check convergence
  - (a) Compute the spacial variance  $\sigma^2(\mathcal{J}) = \sum_{i=2}^{L-1} (\mathcal{J}_i - \bar{\mathcal{J}})^2 / (L-2)$
  - (b) Compute the change with the bond dimension  $\epsilon_\chi = \bar{\mathcal{J}}(\chi_i) - \bar{\mathcal{J}}(\chi_{i-1})$
  - (c) Repeat steps 2,3 and 4 until  $|\sigma(\mathcal{J})/\bar{\mathcal{J}}| < 1\%$  and  $|\epsilon_\chi/\bar{\mathcal{J}}| < 0.5\%$
5. Compute the final current and associated error  $\epsilon_J = \max(\sigma(\mathcal{J}), \epsilon_\chi)$ .

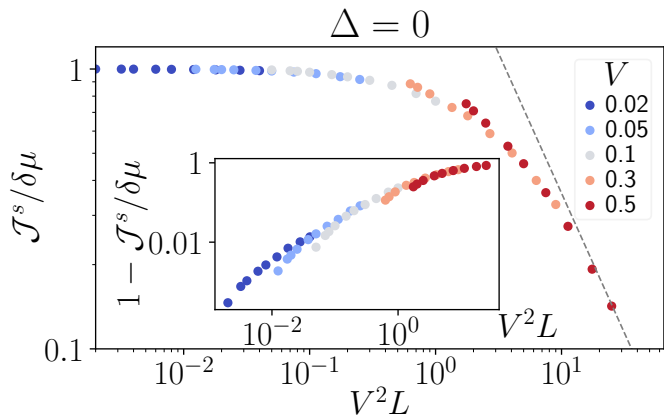


Figure 6. Finite-size scaling of the spin current with the parameter  $V^2L$ . The dashed line corresponds to the asymptotic diffusive regime, Eq. (6). The inset shows also how the scaling with  $V^2L$  fails also for  $V \rightarrow 0$  in describing the deviations from the ballistic regime in which  $\mathcal{J}^s = \delta\mu$ .

In most situations, we require a much stricter bond on the homogeneity condition, often requiring  $|\sigma(\mathcal{J})/\bar{\mathcal{J}}| < 0.1\%$ . The time step of the Trotter decomposition is variable along the algorithm. For small bond dimensions, we use a large time step,  $dt = 0.2$ , to quickly advance the simulation and reduce it when closer to convergence, up to  $dt = 0.05$ . Due to the convergence criterion employed, simulations can take weeks to converge or reach inaccessible bond dimensions. For this reason, if the criterion are not satisfied for  $\chi \leq 160$ , we consider that the system has not converged and do not show it.

The algorithm was implemented using the open-source ITensor library [53].

## Appendix B: Universal Scaling

In this Appendix, we provide further details on the universality of the scaling discussed in Sec. III.

In the sole presence of non-integrable interactions, the current is expected to scale as a universal function controlled by the scattering length  $L^* \sim V^{-2}$ . However, perturbation theory shows that for small/intermediate system sizes ( $L < 15$ ) the scaling parameter must be of the form  $V^2 f_{V^2}(L)$  instead. In Fig. 6, we show how the naive scaling with  $L/L^* \propto V^2L$  fails to produce a perfect collapse of all curves at weak and moderate IB strengths and intermediate system sizes.

It follows from Fick's law that, when imposing a fixed bias, the magnetization profile interpolates linearly between the borders. However, this is only true in the thermodynamic limit, and finite systems present small deviations up to four sites into the chain's bulk. In Fig. 7-top, we depict the magnetization profile of the XX model close to the diffusive regime for different system sizes. The effects of the border are visible up to very large systems,  $L = 100$ .

For consistency, we verify that the magnetization's gradient converges to  $\nabla \langle \sigma^z \rangle = -\delta\mu/L$  in the diffusive regime,  $V^2 f_{V^2}(L) \gg 1$ , see Fig. 7-bottom. There, we depict the rescaled gradient of  $\sigma^z$  obtained by a linear fit of the magnetization close to the middle of the chain. We find an overall scaling with  $V^2 f_{V^2}(L)$  but, in contrast to Fig. 2, the finite size effects in the magnetization profile lead to non-negligible deviations. Close to the ballistic regime, we find a moderate agreement with  $\nabla \langle \sigma^z \rangle = -\frac{\delta\mu}{L} V^2 f_{V^2}(L)$ , depicted as dashed gray line.

### Appendix C: Perturbation Theory

As mentioned in the main text, perturbation theory (PT) provides a benchmark and helpful insights on the numerical data in the limit of small interactions. In this section, we provide further details on the method.

The object of interest is the NESS of the system. It corresponds to the unique (in our case) zero eigenvalue of the non-unitary master equation (4). This equation can be written in terms of the Liouvillian super-operator  $d_t \rho = \mathcal{L}(\rho)$  or, most practically, using the Liouville space formulation

$$\frac{d \|\rho(t)\rangle}{dt} = \hat{\mathcal{L}} \|\rho(t)\rangle, \quad (\text{C1})$$

where  $\|\rho\rangle$  is the row-vectorized form of the density matrix  $\rho$  and the inner product satisfies  $\langle A \| B \rangle = \text{Tr}(A^\dagger B)$ . Super-operators are denoted by a hat.

The first step in PT is to find the eigendecomposition of the unperturbed problem, i.e. the super-operator of the non-interacting boundary-driven XX model,  $\mathcal{L}_{\text{XX}}$ . As a direct consequence of the non-unitarity of general Lindblad evolutions, the Lindblad super-operator is described by a non-hermitian matrix and thus has different left and right eigenvectors,  $\tilde{\rho}_\mu$  and  $\rho_\mu$  respectively. They respect the normalization condition  $\langle \tilde{\rho}_\mu \| \rho_\nu \rangle = \delta_{\mu\nu}$  and share the same eigenvalue  $\lambda_\mu$ , whose real part corresponds to the physical relaxation rate of  $\rho_\mu$ .

The eigenstates of  $\mathcal{L}_{\text{XX}}$  serve as the basis to perturbatively construct the eigenstates of the full problem. Since  $\mathcal{L}_{\text{XX}}$  is a quadratic super-operator, it is useful to rely on the third-quantization formalism [76, 77] to find its eigendecomposition. In Sec. D, we construct the  $4^L$  eigenstates  $\rho_\mu$  by consecutively acting with annihilation(creation) operators,  $c^{(\prime)}$  on a vacuum state of  $2L$  particles. This approach allows to diagonalize the Lindblad super-operator, which can be written as

$$\begin{aligned} \hat{\mathcal{L}}_{\text{XX}} &= \sum_i^{2L} \alpha_i c'_i c_i \\ &= \sum_\mu^{4^L} \lambda_\mu \|\rho_\mu\rangle \langle \tilde{\rho}_\mu|, \end{aligned} \quad (\text{C2})$$

where  $\|\rho_\mu\rangle = \sum_{\{\mu_i\}} c_1^{\mu_1} \dots c_{2L}^{\mu_{2L}} \|0\rangle$  and  $\lambda_\mu = \sum_i^{2L} \mu_i \alpha_i$ . All the models discussed here have a unique

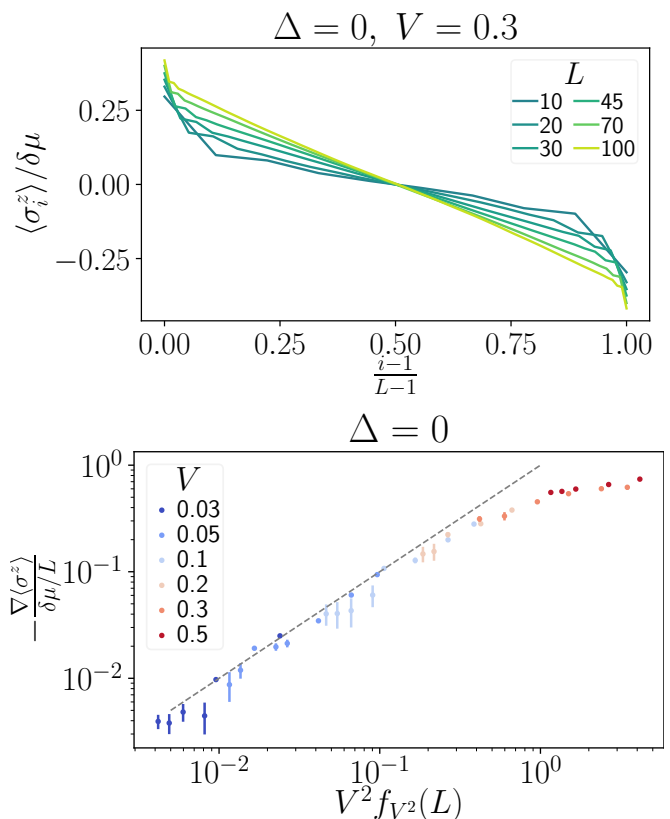


Figure 7. Top) Magnetization profile close to the diffusive regime for different system sizes. Bottom) Rescaled slope of the magnetization for different IB parameters as a function of  $V^2 f_{V^2}(L)$ . System sizes range from  $L = 15$  to  $L = 100$ . Analytic predictions close to the ballistic regime are depicted as dashed lines. In the diffusive regime ( $V^2 f_{V^2}(L) \approx 1$ ), the magnetization slope approaches  $\delta\mu/L$  as expected.

NESS that satisfies  $\lambda_0 = 0$  and  $\tilde{\rho}_0 = \mathbb{I}$ . The NESS of the XX model carries a finite current proportional to the bias,  $\text{Tr}[\hat{\mathcal{J}}^s \rho_0] = \delta\mu$ .

In the second step of PT, we look for a perturbative solution to the NESS of Eq. (4), in the form  $\rho_{ss} = \sum_{m,n=0}^{\infty} V^m \Delta^n \rho^{(m,n)}$ , where  $\rho^{(0,0)} = \rho_0$  is the NESS of the XX model. Assuming orthonormality of left and right eigenvectors, the expansion terms can be computed order by order [78]:

$$\rho^{(m,n)} = i\mathcal{L}_{\text{XX}}^+ \left( [\mathcal{H}_{\text{NNN}}, \rho^{(m-1,n)}] + [\mathcal{H}_{\text{XXZ}}^{J=0}, \rho^{(m,n-1)}] \right), \quad (\text{C3})$$

where we introduced the Moore-Penrose pseudoinverse of the super-operator  $\mathcal{L}_{\text{XX}}(\circ)$ ,  $\mathcal{L}_{\text{XX}}^+(\circ) = \sum_{\mu>0} \lambda_\mu^{-1} \rho_\mu \text{Tr}(\tilde{\rho}_\mu \circ)$ . The above perturbation scheme ensures that at any truncation order, the density matrix remains Hermitian, positive-semidefinite and with trace equal to one [79]. Equation (C3) leads to the same results of the variational approach in Ref. [59].

We analytically compute corrections to the bulk's spin current up to second order in perturbation theory. All the results are valid only in the linear response regime,

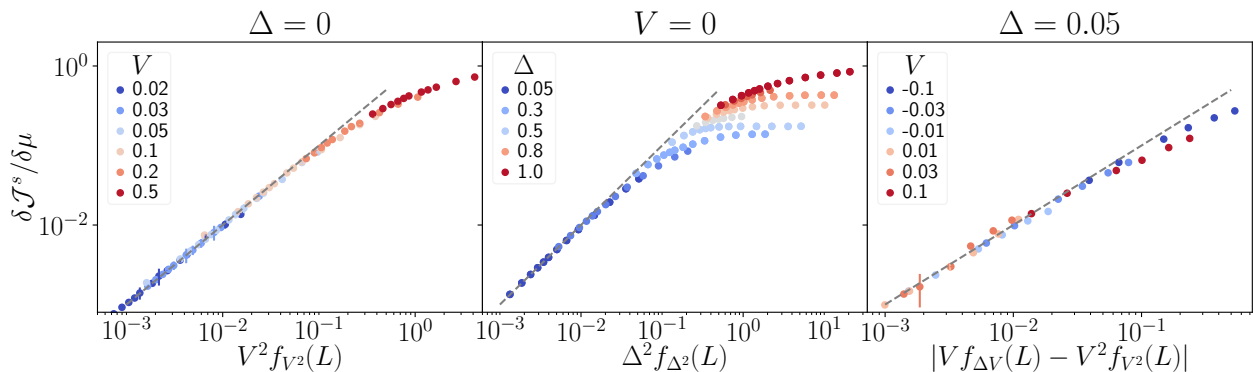


Figure 8. Deviations from the ballistic current for small (next-to)-nearest neighbor interactions. System sizes range from  $L = 5$  to  $L = 100$ . The numerical data closely follows the analytic predictions of (C4) depicted as dashed lines.

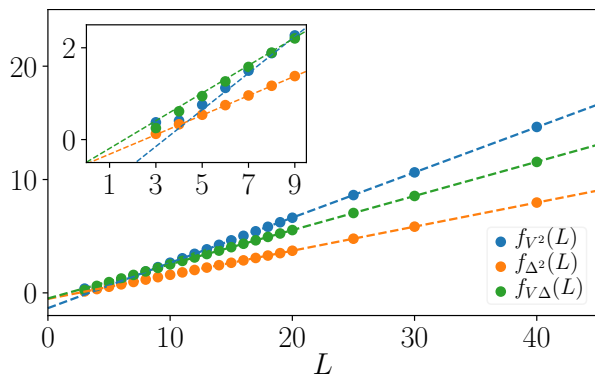


Figure 9. System size dependence of the functions  $f_i$  in Eq. (C4). Dashed lines depict the linear fitting performed beyond  $L = 6$ . Inset: highlight for very short systems, in which the deviations from perfect linear scaling can be appreciated.

$|\delta\mu| \ll 1$  and discard higher order corrections  $\mathcal{O}(\mu^2)$ . Assuming  $\gamma = J = 1$  in Eq. (4), we obtain

$$\begin{aligned} \mathcal{J}^s &= \sum_{m,n=0}^{\infty} V^m \Delta^n \text{Tr} \left( \hat{\mathcal{J}}_s \rho^{(m,n)} \right) \\ &\approx \left[ 1 - V^2 f_{V^2}(L) - \Delta^2 f_{\Delta^2}(L) + V \Delta f_{V\Delta}(L) \right] \delta\mu \end{aligned} \quad (\text{C4})$$

The system size dependence of the functions  $f_{V^2, \Delta^2, V\Delta}$  is shown in Fig. 9. Beyond  $L \sim 5$ , the scaling for all  $f_i$  is linear in  $L$  and the fitting functions  $f_i = a_i L + b_i$  are depicted in corresponding dashed lines and reported in Table I.

	$a$	$b$
$f_{V^2}$	0.3992	-1.348
$f_{\Delta^2}$	0.2124	-0.5307
$f_{V\Delta}$	0.3015	-0.4946

Table I. Fitting parameters of the second order corrections to the current.

Notice the linearity in  $V$  of the third term in Eq. (C4),

which is responsible for the current enhancement. It is clear from Eq. (C4) that the large  $L$  limit and the small interactions limit do not commute. For instance, both the integral and non-integrable corrections to the XX model lead to divergent contributions which do not capture the enforcement of ballistic or diffusive behavior at large system sizes.

We illustrate now the agreement with PT and our tDMRG simulations. In the main text, we compared the PT results against a polynomial fit of the current, see Fig. 5. We argued that Eq. (C4) correctly predicted the current in the limit of  $\Delta \rightarrow 0$  but some small deviations were observed in the order  $\mathcal{O}(V^2)$  term. In Fig. 8, we present a complementary analysis of the data which does not rely on fitting polynomials. Fig. 8 depicts the correction to the current,  $\delta\mathcal{J}^s$ , upon turning on interactions, respectively  $V$ ,  $\Delta$  and  $V$ , for left, center and right plots. The  $x$ -axis is rescaled according to (C4) and dashed gray lines depict the perturbation theory predictions.

We can observe that, for small interactions ( $\Delta$  and  $V$ ), the current is indeed well described by Eq. (C4). As noted in the main text, the presence of a single next-to-nearest neighbor interaction is characterized by a strong scaling of the current with the variable  $V^2 f_{V^2}(L)$ , Fig. 8-left. This is qualitatively different from the nearest neighbor interactions where the current converges to a value independent of  $L$  and a scaling with  $\Delta^2 f_{\Delta^2}(L)$  is never possible, see Fig. 8-center. Nevertheless, we can observe that for small  $\Delta \leq 0.3$  an approximate scaling with  $\Delta^2 f_{\Delta^2}(L)$  might be possible. In that situation, the current would saturate after a length of order  $L_{\Delta} \sim 1/\Delta^2$ . For stronger interactions,  $L_{\Delta}$  appears to diverge close to  $\Delta = 1$  but for  $0.8 > \Delta > 0.3$  the current still saturates before  $\Delta^2 f_{\Delta^2}(L) \lesssim 10$ . Fig. 8-right shows that, for small  $\Delta$ , perturbation theory becomes exact and that the derivations discussed in Fig. 5 are indeed an artifact of the fitting.

### Appendix D: Diagonalization of the XX chain

In this section, we provide a summary on how to diagonalize the non-interacting XX limit,  $V = \Delta = 0$ . We follow the protocol of Ref. [77] which reduces the diagonalization problem to finding the eigenbasis of a  $2L \times 2L$  matrix. It is useful to work in the fermionic representation via the Jordan-Wigner transformation

$$\begin{aligned}\sigma_j^+ &= e^{-i\pi \sum^{j-1} n_k} a_j^\dagger \\ \sigma_j^- &= e^{i\pi \sum^{j-1} n_k} a_j \\ \sigma_j^z &= 2a_j^\dagger a_j - 1\end{aligned}\quad (\text{D1})$$

In the fermionic representation, the Hamiltonian becomes

$$\mathcal{H}_{\text{XX}} = \sum_{i,j=1}^L h_{ij} a_i^\dagger a_j \quad (\text{D2})$$

with  $h_{i,j} = 2J\delta_{|i-j|,1}$ . Since the  $\{a_i, a_i^\dagger\}$  operators act left and right of the density matrix, it is useful to work in the Liouville space of super-operators. In the super-operator formalism, density matrices are mapped onto vectors in a vector space of dimensions  $\mathbb{C}^{4^L} \times \mathbb{C}^{4^L}$  according to the mapping  $\|M\rho N\rangle = M \otimes N^T \|\rho\rangle$ , where  $\|\rho\rangle$  is the row-vectorized form of the matrix  $\rho$ . We can now define a new set of  $2L$  super-operators  $\mathcal{B} = \{b_i, b_i^\dagger, b_{L+i}, b_{L+i}^\dagger\}_{i=1}^L$  which act on  $\|\rho\rangle$  according to:

$$\begin{aligned}b_i \|\rho\rangle &= \|a_i \rho\rangle \\ b_i^\dagger \|\rho\rangle &= \|a_i^\dagger \rho\rangle \\ b_{L+i} \|\rho\rangle &= \|\mathcal{P}(\rho a_i^\dagger)\rangle \\ b_{L+i}^\dagger \|\rho\rangle &= \|\mathcal{P}(\rho) a_i\rangle\end{aligned}\quad (\text{D3})$$

where  $\mathcal{P} = e^{i\pi \sum n_i \otimes \mathbb{I} + \mathbb{I} \otimes n_i^T}$  is a super-operator string which imposes the necessary anti-commutations relations  $\{b_i^\dagger, b_j\} = \delta_{ij}$ . In practice, the  $\mathcal{B}$  basis acts as a complete set of creation and destruction operators in the occupation number basis of a lattice of size  $2L$ . Physically,  $\mathcal{P}$  is a parity operator with eigenvalues  $\pm 1$  and counts the number of excitations in the new fermionic system with  $2L$  states. For reasons clear bellow, we will only be interested in  $\mathcal{P} = 1$ . In the new  $\mathcal{B}$  basis, the Lindblad super-operator reads:

$$\begin{aligned}\hat{\mathcal{L}}_{\text{XX}} &= -i \sum_{i,j=1}^L \left( h_{i,j} b_i^\dagger b_j - h_{j,i} b_{L+i}^\dagger b_{L+j} \right) \\ &+ \sum_{i=1,L} \Gamma(1 + \mu_i) \left( 2b_i^\dagger b_{L+i}^\dagger \mathcal{P} - b_{L+i} b_{L+i}^\dagger - b_i b_i^\dagger \right) \\ &+ \sum_{i=1,L} \Gamma(1 - \mu_i) \left( -2b_i b_{L+i} \mathcal{P} - b_{L+i}^\dagger b_{L+i} - b_i^\dagger b_i \right)\end{aligned}\quad (\text{D4})$$

Similarly to the diagonalization procedure of quadratic Hamiltonians, we are interested in finding a basis of  $2L$  creation and annihilation super-operators  $\mathcal{C} = \{c'_i, c_i\}_{i=1}^{2L}$  that diagonalizes the unperturbed problem,  $\hat{\mathcal{L}}_{\text{XX}} = \sum_{i=1}^{2L} \alpha_i \hat{c}'_i \hat{c}_i$ . If such basis exists, the eigenstates of  $\hat{\mathcal{L}}_{\text{XX}}$  can be constructed from excitations on the vacuum state of the  $c$ 's operators,  $\|\rho_\mu\rangle = \sum_{\{\mu_i\}} c'_1{}^{\mu_1} \dots c'_{2L}{}^{\mu_{2L}} \|0\rangle$  and  $\lambda_\mu = \sum_i^L (\mu_i \alpha_i + \mu_{L+i} \alpha_i^*)$ . Trivially, the NESS is the vacuum state of the  $\mathcal{C}$  basis.

Due to particle hole symmetry, the values of  $\alpha_i$  must come in conjugate pares  $\{\alpha, \alpha^*\}$  with  $\Re(\alpha) \leq 0$ . We fix  $\alpha_i^* = \alpha_{L+i}$  in our notation. In general, the Lindblad super-operator is not hermitian and neither are the  $c$ 's super-operators, however they still respect the fermionic anti-commutation relations  $\{c_i, c'_j\} = \delta_{i,j}$  and  $\{c_i, c_j\} = \{c'_i, c'_j\} = 0$ . The  $c, c'$  operators represent a linear super position of particle and hole excitations acting both left and right of the density matrix and should be understood as the “normal modes” of the open system. The exact mapping between  $\{c_i, c'_j\}$  and  $\{b_i, b_i^\dagger\}$  operators can be found in Ref.[77] and shown here for completeness

$$\begin{bmatrix} b_{1 \rightarrow L} \\ b_{L+1 \rightarrow 2L}^\dagger \\ b_{1 \rightarrow L}^\dagger \\ b_{L+1 \rightarrow 2L} \end{bmatrix} = \begin{bmatrix} W & 0 \\ 0 & -Y_L W^* Y_L \end{bmatrix} \begin{bmatrix} c_{1 \rightarrow L} \\ c'_{L+1 \rightarrow 2L} \\ c'_{1 \rightarrow L} \\ c_{L+1 \rightarrow 2L} \end{bmatrix} \quad (\text{D5})$$

where  $Y_L = -i \begin{bmatrix} 0 & \mathbb{I}_L \\ -\mathbb{I}_L & 0 \end{bmatrix}$  and the columns of  $W$  are the right eigenvectors of a matrix  $M$ . In our work,  $M$  acquires a simple form

$$M = \frac{1}{2} \begin{bmatrix} -ih + \Lambda^+ - \Lambda^- & 2\Lambda^+ \\ 2\Lambda^- & -ih - \Lambda^+ + \Lambda^- \end{bmatrix} \quad (\text{D6})$$

with diagonal matrices  $\Lambda_i^+ = (\delta_{i,1} + \delta_{i,L})\Gamma(1 + \mu_i)$  and  $\Lambda_i^- = (\delta_{i,1} + \delta_{i,L})\Gamma(1 - \mu_i)$ .

To our knowledge, there is no analytical solution for  $W$  as a function of  $L$  and so we resort to exact diagonalization. Once the mapping of Eq. (D5) is found, we can express any super-operator in the  $\mathcal{C}$  basis.

- 
- [1] J. M. Deutsch, *Physical Review A* **43**, 2046 (1991).
- [2] M. Srednicki, *Physical Review E* **50**, 888 (1994).
- [3] M. Rigol, V. Dunjko, and M. Olshanii, *Nature* **452**, 854 (2008), [arXiv:0708.1324](#).
- [4] L. D'Alessio, Y. Kafri, A. Polkovnikov, and M. Rigol, *Advances in Physics* **65**, 239 (2016).
- [5] T. Kinoshita, T. Wenger, and D. S. Weiss, *Nature* **440**, 900 (2006).
- [6] O. A. Castro-Alvaredo, B. Doyon, and T. Yoshimura, *Physical Review X* **6**, 041065 (2016), [arXiv:1605.07331](#).
- [7] B. Bertini, M. Collura, J. De Nardis, and M. Fagotti, *Physical Review Letters* **117** (2016), 10.1103/PhysRevLett.117.207201, [arXiv:1605.09790](#).
- [8] M. Rigol, V. Dunjko, V. Yurovsky, and M. Olshanii, *Physical Review Letters* **98**, 050405 (2007), [arXiv:0604476 \[cond-mat\]](#).
- [9] E. Ilievski and J. De Nardis, *Physical Review Letters* **119**, 020602 (2017).
- [10] S. Gopalakrishnan and R. Vasseur, *Physical Review Letters* **122**, 127202 (2019).
- [11] T. Prosen, *Physical Review Letters* **106**, 2 (2011), [arXiv:1103.1350](#).
- [12] M. Ljubotina, M. Žnidarič, and T. Prosen, *Nature Communications* **8**, 1 (2017), [arXiv:1702.04210](#).
- [13] B. Bertini, F. Heidrich-Meisner, C. Karrasch, T. Prosen, R. Steinigeweg, and M. Žnidarič, [arXiv:2003.03334 \[cond-mat, physics:quant-ph\]](#) (2020).
- [14] Y. Tang, W. Kao, K.-Y. Li, S. Seo, K. Mallayya, M. Rigol, S. Gopalakrishnan, and B. L. Lev, *Physical Review X* **8**, 021030 (2018).
- [15] K. Mallayya, M. Rigol, and W. De Roeck, *Physical Review X* **9**, 021027 (2019).
- [16] A. J. Friedman, S. Gopalakrishnan, and R. Vasseur, *Physical Review B* **101**, 180302 (2020).
- [17] J. Durnin, M. J. Bhaseen, and B. Doyon, [arXiv:2004.11030 \[cond-mat\]](#) (2020).
- [18] F. Möller, C. Li, I. Mazets, H.-P. Stimming, T. Zhou, Z. Zhu, X. Chen, and J. Schmiedmayer, [arXiv:2006.08577 \[cond-mat\]](#) (2020).
- [19] P. Jung, R. W. Helmes, and A. Rosch, *Physical Review Letters* **96**, 067202 (2006), [arXiv:0509615 \[cond-mat\]](#).
- [20] V. B. Bulchandani, C. Karrasch, and J. E. Moore, *Proceedings of the National Academy of Sciences* (2020), 10.1073/pnas.1916213117.
- [21] P. G. Silvestrov, *Physical Review E - Statistical Physics, Plasmas, Fluids, and Related Interdisciplinary Topics* **58**, 5629 (1998).
- [22] C. Neuenhahn and F. Marquardt, *Physical Review E - Statistical, Nonlinear, and Soft Matter Physics* **85**, 060101 (2012).
- [23] M. Pandey, P. W. Claeys, D. K. Campbell, A. Polkovnikov, and D. Sels, [arXiv preprint arXiv:2004.05043](#) (2020).
- [24] M. Brenes, E. Mascarenhas, M. Rigol, and J. Goold, *Physical Review B* **98**, 235128 (2018).
- [25] M. Brenes, T. LeBlond, J. Goold, and M. Rigol, (2020), [arXiv:2004.04755](#).
- [26] M. Brenes, J. Goold, and M. Rigol, [arXiv:2005.12309 \[cond-mat\]](#) (2020).
- [27] D. J. Luitz and Y. Bar Lev, *Physical Review Letters* **117**, 170404 (2016).
- [28] F. H. L. Essler and M. Fagotti, *Journal of Statistical Mechanics: Theory and Experiment* **2016**, 064002 (2016).
- [29] P. Calabrese and J. Cardy, *Journal of Statistical Mechanics: Theory and Experiment* **2016**, 064003 (2016).
- [30] D. Bernard and B. Doyon, *Journal of Statistical Mechanics: Theory and Experiment* **2016**, 064005 (2016).
- [31] J. De Nardis, D. Bernard, and B. Doyon, *Physical Review Letters* **121**, 160603 (2018).
- [32] A. Biella, M. Collura, D. Rossini, A. De Luca, and L. Mazza, *Nature Communications* **10**, 4820 (2019), [arXiv:1905.00088](#).
- [33] C. W. Von Keyserlingk, T. Rakovszky, F. Pollmann, and S. L. Sondhi, *Physical Review X* **8**, 21013 (2018), [arXiv:1705.08910](#).
- [34] V. Alba and P. Calabrese, *Physical Review B* **100**, 115150 (2019), [arXiv:1903.09176](#).
- [35] S. Jesenko and M. Žnidarič, *Physical Review B - Condensed Matter and Materials Physics* **84**, 174438 (2011).
- [36] S. Trotzky, Y.-A. Chen, A. Flesch, I. P. McCulloch, U. Schollwöck, J. Eisert, and I. Bloch, *Nature Physics* **8**, 325 (2012).
- [37] M. Gring, M. Kuhnert, T. Langen, T. Kitagawa, B. Rauer, M. Schreitl, I. Mazets, D. A. Smith, E. Demler, and J. Schmiedmayer, *Science* **337**, 1318 (2012), [arXiv:1112.0013](#).
- [38] S. Hofferberth, I. Lesanovsky, B. Fischer, T. Schumm, and J. Schmiedmayer, *Nature* **449**, 324 (2007).
- [39] N. Jepsen, J. Amato-Grill, I. Dimitrova, W. W. Ho, E. Demler, and W. Ketterle, [arXiv:2005.09549 \[cond-mat\]](#) (2020).
- [40] U. Schollwöck, *Reviews of Modern Physics* **77**, 259 (2005), [arXiv:0409292 \[cond-mat\]](#).
- [41] S. R. White, *Physical Review Letters* **102**, 190601 (2009), [arXiv:arXiv:0902.4475v2](#).
- [42] S. R. White, *Physical Review Letters* **69**, 2863 (1992).
- [43] D. Perez-Garcia, F. Verstraete, M. M. Wolf, and J. I. Cirac, *Quantum Information and Computation* **7**, 401 (2007), [arXiv:0608197 \[quant-ph\]](#).
- [44] D. M. Kennes and C. Karrasch, *Computer Physics Communications* **200**, 37 (2016).
- [45] M. Žnidarič, *Physical Review B* **99**, 035143 (2019).
- [46] S. Krinner, D. Stadler, D. Husmann, J.-P. Brantut, and T. Esslinger, *Nature* **517**, 64 (2015).
- [47] J.-P. Brantut, C. Grenier, J. Meineke, D. Stadler, S. Krinner, C. Kollath, T. Esslinger, and A. Georges, *Science* **342**, 713 (2013).
- [48] M. Lebrat, P. Grišins, D. Husmann, S. Häusler, L. Cormann, T. Giamarchi, J.-P. Brantut, and T. Esslinger, *Physical Review X* **8**, 011053 (2018).
- [49] H. Bethe, *Zeitschrift für Physik* **71**, 205 (1931).
- [50] V. Gorini, A. Kossakowski, and E. C. G. Sudarshan, *Journal of Mathematical Physics* **17**, 821 (1976).
- [51] G. Lindblad, *Communications in Mathematical Physics* **48**, 119 (1976).
- [52] If the boundary spins that are connected to the jump operators were to be isolated from the chain's bulk, their occupation would be  $\mu_\alpha \leq 1$ .
- [53] [ITensor Library \(version 2.1.1\)](#).
- [54] M. Žnidarič, *Journal of Statistical Mechanics: Theory and Experiment* **2010** (2010), 10.1088/1742-5468/2010/05/L05002, [arXiv:1005.1271](#).

- [55] M. Žnidarič, *Journal of Physics A: Mathematical and Theoretical* **43** (2010), 10.1088/1751-8113/43/41/415004, arXiv:1006.5368.
- [56] The general expression for different injections rates  $\gamma_{L/R} \neq 1$  on the left and on the right of the chain reads  $\mathcal{J}^s = \delta\mu \cdot 4\gamma_L\gamma_R / [(1 + \gamma_L\gamma_R)(\gamma_L + \gamma_R)]$  [55].
- [57] X. Zotos, F. Naef, and P. Prelovsek, *Physical Review B* **55**, 11029 (1997).
- [58] X. Zotos, *Physical Review Letters* **82**, 1764 (1999).
- [59] M. Žnidarič, *Physical Review Letters* **106** (2011), 10.1103/PhysRevLett.106.220601, arXiv:1103.4094.
- [60] R. J. Sánchez, V. K. Varma, and V. Oganesyan, *Physical Review B* **98**, 054415 (2017), arXiv:1711.11214.
- [61] The parameter  $c_2$  deviates slightly from PT results in the  $\Delta \rightarrow 0$ . This is an artifact of the fitting procedure as argued in App. B.
- [62] M. Znidaric, arXiv:2006.09793 [cond-mat, physics:nlin, physics:quant-ph] (2020), arXiv: 2006.09793.
- [63] V. Eisler, *Journal of Statistical Mechanics: Theory and Experiment* **2011**, P06007 (2011), publisher: IOP Publishing.
- [64] M. Žnidarič and M. Horvat, *The European Physical Journal B* **86**, 67 (2013).
- [65] J. J. Mendoza-Arenas, M. Žnidarič, V. K. Varma, J. Goold, S. R. Clark, and A. Scardicchio, *Physical Review B* **99**, 094435 (2019), arXiv:1803.11555.
- [66] N. W. Ashcroft, *Solid State Physics* (Thomson Press, New Delhi, 2003).
- [67] C. L. Kane and M. P. A. Fisher, *Physical Review Letters* **76**, 3192 (1996).
- [68] R. Fazio, F. W. J. Hekking, and D. E. Khmelnitskii, *Physical Review Letters* **80**, 5611 (1998).
- [69] M. Filippone, P. W. Brouwer, J. Eisert, and F. von Oppen, *Physical Review B* **94**, 201112 (2016).
- [70] G. Salerno, H. M. Price, M. Lebrat, S. Häusler, T. Esslinger, L. Corman, J.-P. Brantut, and N. Goldman, *Physical Review X* **9**, 041001 (2019).
- [71] M. Filippone, C.-E. Bardyn, S. Greschner, and T. Giamarchi, *Physical Review Letters* **123**, 086803 (2019).
- [72] S. Greschner, M. Filippone, and T. Giamarchi, *Physical Review Letters* **122**, 083402 (2019), arXiv:1809.10927.
- [73] T. Prosen and M. Žnidarič, *Journal of Statistical Mechanics: Theory and Experiment* **2009**, P02035 (2009), arXiv:0811.4188.
- [74] T. Prosen and I. Pižorn, *Journal of Physics A: Mathematical and General* **39**, 5957 (2006), arXiv:0602074 [quant-ph].
- [75] A. J. Daley, *Manipulation and Simulation of Cold Atoms in Optical Lattices*, Ph.D. thesis, Leopold-Franzens-Universität Innsbruck (2005).
- [76] T. Prosen, *New Journal of Physics* **10**, 043026 (2008).
- [77] C. Guo and D. Poletti, *Physical Review A* **95**, 052107 (2017), arXiv:1609.07838.
- [78] A. C. Li, F. Petruccione, and J. Koch, *Scientific Reports* **4**, 4887 (2014), arXiv:1311.3227.
- [79] This is not true in general and comes from the fact that we perturb by adding a Hamiltonian term.